Mutations in *SPATA5* Are Associated with Microcephaly, Intellectual Disability, Seizures, and Hearing Loss

Akemi J. Tanaka,[1] Megan T. Cho,[2] Francisca Millan,[2] Jane Juusola,[2] Kyle Retterer,[2] Charuta Joshi,[3] Dmitriy Niyazov,[4] Adolfo Garnica,[5] Edward Gratz,[6] Matthew Deardorff,[7] Alisha Wilkins,[7] Xilma Ortiz-Gonzalez,[8] Katherine Mathews,[3] Karin Panzer,[9] Eva Brilstra,[10] Koen L.I. van Gassen,[10] Catharina M.L. Volker-Touw,[10] Ellen van Binsbergen,[10] Nara Sobreira,[11] Ada Hamosh,[11] Dianalee McKnight,[2] Kristin G. Monaghan,[2] and Wendy K. Chung[1,12],*

Using whole-exome sequencing, we have identified in ten families 14 individuals with microcephaly, developmental delay, intellectual disability, hypotonia, spasticity, seizures, sensorineural hearing loss, cortical visual impairment, and rare autosomal-recessive predicted pathogenic variants in spermatogenesis-associated protein 5 (*SPATA5*). *SPATA5* encodes a ubiquitously expressed member of the ATPase associated with diverse activities (AAA) protein family and is involved in mitochondrial morphogenesis during early spermatogenesis. It might also play a role in post-translational modification during cell differentiation in neuronal development. Mutations in *SPATA5* might affect brain development and function, resulting in microcephaly, developmental delay, and intellectual disability.

Whole-exome sequencing (WES) is an emerging clinical tool for identifying genes associated with genetically heterogeneous disorders, such as global developmental delay,[1] intellectual disability (ID),[2] schizophrenia,[3] and epilepsy.[4] In individuals in whom initial diagnostic workup and genetic evaluation are unrevealing and without specific clinical features to suggest a diagnosis, WES with the inclusion of parents can be a powerful tool for identifying de novo and inherited rare variants.[1,5] Here, we describe 14 individuals who are from ten independent families and who have homozygous or compound-heterozygous rare variants that are predicted to be deleterious. *SPATA5* (MIM: 613940; GenBank: NM_145207.2) is located in chromosomal region 4q28.1 and encodes a member of the ATPase associated with diverse activities (AAA) protein family. Common features in these individuals include microcephaly, ID, generalized intractable epilepsy, hypotonia, spasticity, sensorineural hearing loss, and cortical visual defects.

Clinical WES was performed on 3,359 individuals with developmental delay, ID, or seizures in one clinical laboratory. In ten affected children from seven unrelated families, we identified variants in *SPATA5* as potentially causative for the phenotype. Through GeneMatcher,[6] we identified four additional probands from three families, giving us a total of 14 affected children in ten families. Twelve of the individuals are of European descent, and two (individuals 6 and 7) are Hispanic. All of the families were sequenced with WES performed in either a

proband-parent trio analysis or a family analysis using affected or unaffected siblings in the segregation analysis (Figure S2). Informed consent was obtained for each individual.

Genomic DNA was extracted from whole blood from the affected children and their parents. Exome sequencing at GeneDx was performed on exon targets isolated by capture with the Agilent SureSelect Human All Exon V4 (50 Mb) Kit (Agilent Technologies). One microgram of DNA from blood specimen was sheared into 350- to 400-bp fragments, which were then repaired, ligated to adaptors, and purified for subsequent PCR amplification. Amplified products were then captured by biotinylated RNA library baits in solution according to the manufacturer's instructions. Bound DNA was isolated with streptavidin-coated beads and re-amplified. The final isolated products were sequenced with the Illumina HiSeq 2000 or 2500 sequencing system with 100-bp paired-end reads. At the time of sequencing, DNA sequence was mapped to the reference human genome sequence (UCSC Genome Browser hg19) with the latest internally validated version of the Burrows-Wheeler Aligner (BWA), progressing from BWA v.0.5.8 to BWA-Mem v.0.7.8.[7,8] Targeted coding exons and splice junctions of known protein-coding RefSeq genes were assessed for average depth of coverage, and a minimum depth of 10× was required for inclusion in downstream analysis. Local realignment around insertion-deletion sites was performed with the Genome Analysis Toolkit v.1.6.[9] Variant calls were generated

---

[1]Department of Pediatrics, Columbia University Medical Center, New York, NY 10032, USA; [2]GeneDx, Gaithersburg, MD 20877, USA; [3]Departments of Pediatrics and Neurology, University of Iowa Children's Hospital, Iowa City, IA 52242, USA; [4]Department of Pediatrics, Division of Medical Genetics, Ochsner Health System, New Orleans, LA 70121, USA; [5]Arkansas Children's Hospital, Little Rock, AR 72202, USA; [6]Child Neurology, Gratz & Shafrir, M.D., Baltimore, MD 21215, USA; [7]Department of Pediatrics, Division of Human Genetics, Children's Hospital of Philadelphia, Philadelphia, PA 19104, USA; [8]Departments of Pediatrics and Neurology, Children's Hospital of Philadelphia, University of Pennsylvania School of Medicine, Philadelphia, PA 19104, USA; [9]Department of Pediatrics, University of Iowa Children's Hospital, Iowa City, IA 52242, USA; [10]Department of Medical Genetics, University Medical Center Utrecht, Utrecht 3584, the Netherlands; [11]McKusick-Nathans Institute of Genetic Medicine, Johns Hopkins University, Baltimore, MD 21287, USA; [12]Department of Medicine, Columbia University Medical Center, New York, NY 10032, USA
*Correspondence: wkc15@columbia.edu

simultaneously on all sequenced family members with SAMtools v.0.1.18.[10] All coding exons and surrounding intron-exon boundaries were analyzed. Automated filtering removed common sequence changes (defined as >10% frequency present in 1000 Genomes). The targeted coding exons and splice junctions of the known protein-coding RefSeq genes were assessed for the average depth of coverage and data-quality threshold values. WES data for all sequenced family members were analyzed with GeneDx's XomeAnalyzer (a variant annotation, filtering, and viewing interface for WES data), which includes nucleotide and amino acid annotations, population frequencies (from the NHLBI Exome Sequencing Project Exome Variant Server and 1000 Genomes), in silico prediction tools, amino acid conservation scores, and mutation references. Variants were filtered on the basis of inheritance patterns, lists of genes of interest, and phenotype and population frequencies, as appropriate. Resources including the Human Gene Mutation Database, 1000 Genomes, the NHLBI Exome Variant Server, OMIM, PubMed, and ClinVar were used for evaluating genes and detecting sequence changes of interest. Additional searches were performed with specific lists of genes related to ID. Identified sequence changes of interest were confirmed in all members of the trio by conventional di-deoxy DNA sequence analysis on an ABI3730 (Life Technologies) according to standard protocols with an additional DNA preparation.

To design the prioritization strategy, we used the PhenoDB Variant Analysis Tool[6] to analyze the exomes sequenced at the Baylor-Hopkins Center for Mendelian Genomics. We prioritized rare functional variants (missense variants, nonsense variants, splice-site variants, and indels) that were homozygous, compound heterozygous, or in the proband but not in the unaffected sibling and excluded variants with a minor allele frequency > 0.01 in dbSNP builds 126, 129, and 131, the Exome Variant Server (release ESP6500SI-V2), or 1000 Genomes. We also excluded all variants found in our in-house control individuals (CIDRVar 51 Mb). With that, we generated lists of homozygous and compound-heterozygous variants for the affected siblings.

The exomes sequenced in the Netherlands were enriched with the SureSelect XT Human All Exon V5 Kit (Agilent) and sequenced in rapid mode on the HiSeq 2500 sequencing system (Illumina) at a mean target depth of 100× (target defined as coding exons in the UCSC Genome Browser and Ensembl ± 20-bp intron flanks). At this depth, >95% of the target was covered at >10×. Detected variants were annotated and filtered with the Bench Lab NGS platform (Cartagenia). Probably deleterious SPATA5 variants consistent with autosomal-recessive inheritance were identified in both individuals. After matches were identified in the GeneMatcher database, these variants were reported as potentially causative mutations.

Exome sequencing from seven affected childrens' samples analyzed at the original clinical laboratory produced an average of ~11 Gb of sequence per sample. Mean coverage of the captured regions was ~140× per sample, >98% was covered at >10× coverage, an average of >92% of base call quality scores were ≥Q30, and the overall mean quality score was >Q36. When we considered all possible modes of inheritance, filtering of common SNPs (>10% frequency in 1000 Genomes) resulted in ~5,400 variants per proband sample in 548 genes (974 unique sequence changes) of interest identified across seven families (Table S1). We evaluated each of these 548 genes by variant allele frequency in reference populations, known disease association, pattern of inheritance, and similarity of clinical phenotype, leaving one gene of interest: SPATA5 (Table S1). Variants were confirmed by Sanger sequencing. All 15 variants identified in the ten families are rare and highly conserved throughout evolution. Eight of the variants are predicted to be deleterious by PolyPhen-2, SIFT, CADD, MetaSVM, and MutationTaster (Table 1). The c.251G>A (p.Arg84Gln), c.1343C>T (p.Ser448Leu), c.989_991del (p.Thr330del), c.1883A>G (p.Asp628Gly), and splice c.1714+1G>A variants were each detected in the Exome Aggregation Consortium (ExAC) Browser with an allele frequency of <1/10,000 (Table 1). No other variants are present in the ExAC Browser, 1000 Genomes, Exome Variant Server, or dbSNP. No homozygous loss-of-function variants were detected in the ExAC Browser, 1000 Genomes, Exome Variant Server, or our own internal database of 15,716 exomes. Only one person had a homozygous variant, and all other individuals had compound-heterozygous variants. There were nine missense mutations, three frameshift mutations, one in-frame deletion, one nonsense mutation, and one splice-site mutation. The c.556C>T (p.Arg186*) and c.251G>A (p.Arg84Gln) mutations were each identified independently in two unrelated families. The c.556C>T mutation was part of a shared haplotype. In all families, parents were heterozygous, and the unaffected siblings of individual 5 were each heterozygous for either the c.298G>A (p.Ala100Thr) or the c.556C>T (p.Arg186*) variant, supporting autosomal-recessive inheritance.

Fourteen individuals from ten independent families share similar clinical features, including microcephaly, neurodevelopmental delay, seizures, and sensorineural hearing loss (Tables 2 and S2). The children range in age from 2 to 19 years, and all have moderate to severe ID. All 14 individuals had abnormal electroencephalograms with generalized intractable epilepsy, including tonic clonic, myoclonic, and absence seizures, as well as staring spells. Twelve of the 14 individuals have hypotonia, three have hypertonia, and seven have spasticity. Vision is variably impaired in 14 children and includes cortical visual impairment in seven. Hearing is impaired in all 14 of the children, nine of whom have congenital bilateral sensorineural hearing loss and three of whom have acquired bilateral sensorineural hearing loss. Notably, speech did not improve in one child whose hearing was corrected.

Table 1. Predicted Pathogenicity and Allele Frequencies of *SPATA5* Variants

Amino Acid Change	Chromosome 4 Coordinates	Nucleotide Change	SIFT	PROVEAN	PolyPhen-2	MutationTaster	MetaSVM	CADD Phred	Allele Frequency			
---	---	---	---	---	---	---	---	---	ExAC	1000 Genomes	EVS	XomeDx
p.Arg84Gln	123848876G>A	c.251G>A	tolerated (0.111)	neutral (−0.653)	possibly damaging (0.849)	disease causing (0.39392)	deleterious (0.88398)	22.30	0.00004118	0	0	0.0003
p.Ser90Ile	123848894G>T	c.269G>T	damaging (0.001)	neutral (−2.020)	possibly damaging (0.873)	disease causing (0.34117)	deleterious (0.86851)	17.76	0	0	0	0.0001
p.Ala100Thr	123850204G>A	c.298G>A	damaging (0.002)	neutral (−2.020)	damaging (0.960)	disease causing (0.997)	deleterious (0.90678)	27.60	0	0	0	0.0001
p.Arg186*	123855302C>T	c.556C>T	NA	NA	NA	disease causing (0.70825)	NA	37.00	0	0	0	0.0001
p.Thr330del	123855735_ 123855737del	c.989_991del	NA	deleterious (−4.557)	damaging	disease causing	unknown	22.40	0.0001334	0	0	0
p.Ser448Leu	123859289C>T	c.1343C>T	damaging (0.001)	deleterious (−4.648)	possibly damaging (0.672)	disease causing (0.35151)	deleterious (0.97264)	24.40	0.00002471	0	0	0.0001
p.Asn525Thrfs*20	123868503_ 123868507del	c.1574_1578delATGCT	NA	NA	NA	NA	NA	NA	0	0	0	0.0001
p.Arg529Gln	123868515G>A	c.1586G>A	damaging (0.000)	deleterious (−3.731)	damaging (0.985)	disease causing (0.70825)	deleterious (0.99505)	34.00	0.00002471	0	0	0.0001
p.Tyr559*	123868606C>A	c.1677C>A	NA	NA	damaging	disease causing	unknown	37.00	0	0	0	0
NA	123868644G>A	c.1714+1G>A	NA	NA	unknown	disease causing (1.000)	unknown	16.40	0.0001341	0	0.00015378	0
p.Trp626Cys	123949349G>C	c.1878G>C	damaging (0.000)	deleterious (−12.091)	damaging (0.946)	disease causing (0.40733)	deleterious (0.99215)	21.90	0	0	0	0
p.Asp628Gly	123949354A>G	c.1883A>G	damaging (0.001)	deleterious (−6.762)	damaging (0.97)	disease causing (0.70825)	deleterious (0.99139)	32.00	0.00003295	0	0	0.0001
p.Arg784Gln	124177181G>A	c.2351G>A	damaging (0.001)	deleterious (−3.835)	damaging (0.971)	disease causing (0.40733)	deleterious (0.99177)	21.80	0	0	0	0.0001
p.Ile788Serfs*47	124177192_ 124177201del	c.2362_ 2371delATTGATAGAA	NA	NA	NA	NA	NA	NA	0	0	0	0.0001
p.Ala844Val	124235068C>T	c.2531C>T	tolerated (0.085)	deleterious (−3.512)	possibly damaging (0.723)	disease causing (0.3652)	deleterious (0.95928)	24.80	0	0	0	0.0001

The following abbreviation is used: NA, not applicable.

Table 2.   Clinical Features of Individuals with Mutations in SPATA5

Individual	Age (Years)	Sex	Proband or Sibling	Nucleotide and Amino Acid Changes	Hypotonia	Spasticity	DD	Vision Defect	SNHL	Microcephaly	Brain MRI	Seizure	Abnormal EEG	GI
1	6	F	P	c.2531C>T (p.Ala844Val), c.1574_1578delATGCT (p.Asn525Thrfs*20)	+	+	+	+	+	+	thin corpus callosum	−	+	+
2	9	F	S of 1	c.2531C>T (p.Ala844Val), c.1574_1578delATGCT (p.Asn525Thrfs*20)	+	+	+	+	+	+	thin corpus callosum	+	+	+
3	5	F	P	c.2362_2371delATTGATAGAA (p.Ile788Serfs*47), c.251G>A (p.Arg84Gln)	+	+	+	+	+	+	delayed myelination	+	+	+
4	4	F	P	c.1343C>T (p.Ser448Leu), c.556C>T (p.Arg186*)	+	−	+	+	+	+	normal	+	+	+
5	2	F	P	c.298G>A (p.Ala100Thr), c.556C>T (p.Arg186*)	+	+	+	+	+	+	hypomyelination	+	+	+
6	11	M	P	c.2351G>A (p.Arg784Gln), c.269G>T (p.Ser90Ile)	+	+	+	+	+	+	progressive diffuse atrophy	+	+	+
7	6	F	S of 6	c.2351G>A (p.Arg784Gln), c.269G>T (p.Ser90Ile)	+	−	+	ND	+	+	normal	+	+	+
8	19	M	P	c.1883A>G (p.Asp628Gly), c.1586G>A (p.Arg529Gln)	+	+	+	+	+	ND	cortical atrophy, immature myelination	+	+	+
9	14	F	S of 8	c.1883A>G (p.Asp628Gly), c.1586G>A (p.Arg529Gln)	+	−	+	+	+	+	ND	+	+	−
10	8	M	P	c.1878G>C (p.Trp626Cys), c.1714+1G>A	hypertonia	+	+	+	+	+	normal	+	+	+
11	3	M	S of 10	c.1878G>C (p.Trp626Cys), c.1714+1G>A	+	−	+	+	+	+	ND	+	+	+
12	5	M	P	c.1883A>G (p.Asp628Gly), c.1677C>A (p.Tyr559*)	+	+	+	+	+	−	enlarged cerebrospinal fluid spaces	+	+	+
13	11	F	P	c.989_991del (p.Thr330del)	+	−	+	+	+	+	normal	+	+	+
14	4	M	P	c.251G>A (p.Arg84Gln)	+	+	+	+	+	+	normal	+	+	+

See Table S2 for additional details of clinical presentations. Abbreviations are as follows: DD, developmental delay; EEG, electroencephalogram; GI, gastrointestinal issues; ND, not determined because of availability or applicability; P, proband; S, sibling; SNHL, sensorineural hearing loss.

Microcephaly was observed in at least 12 individuals, four of whom have congenital microcephaly and another four of whom have acquired microcephaly. A single 5-year-old child has a history of developmental regression. Brain MRI was performed and demonstrated abnormalities in seven of the individuals as diffuse atrophy, cortical atrophy, thin corpus callosum, and hypomyelination (Figure S1). Four of the individuals have scoliosis, and four children also have hip dysplasia or hip dislocations. Two individuals have short stature, six have shown failure to thrive, and six require feeding by a gastrostomy tube. Gastrointestinal issues include gastrointestinal reflux disease in four of the children and constipation in three. Thrombocytopenia was observed in three of the individuals, and four are also immunodeficient. Individual 2 is being monitored by an immunologist for dysgamma-globulinemia and is being treated with intravenous immunoglobulin. Generally, the individuals do not have dysmorphic features.

For individuals 3 and 14, muscle biopsies revealed a possible mitochondrial disorder. Electron microscopy demonstrated enlarged and abnormally shaped mitochondria in individual 3. Individual 14's muscle biopsy showed intermyofibrillar linear mitochondrial aggregates, a mild increase in subsarcolemmal and intermyofibrillar mitochondria, and reduced electron transport chain activity, possibly indicating mitochondrial dysfunction.
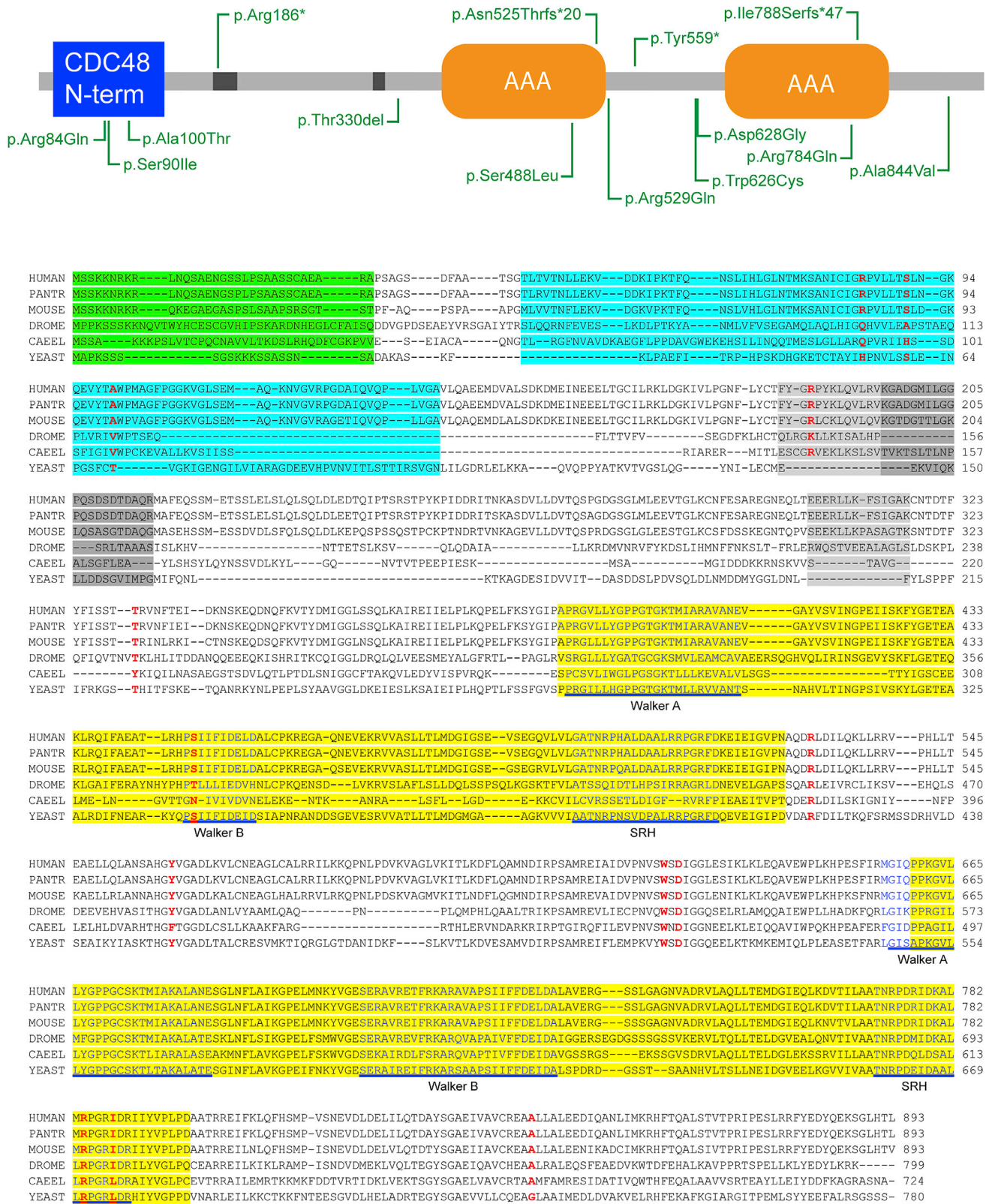
We describe a clinical syndrome characterized by severe neurological impairment including ID, generalized intractable epilepsy, microcephaly, abnormal muscle tone, and sensorineural hearing loss due to autosomal-recessive pathogenic variants in SPATA5. Although they were not observed in every person, cortical visual impairment, problems with feeding and growth, spasticity, scoliosis, immunodeficiency, and thrombocytopenia were also common features (Table S2).

All of our individuals have mutations in SPATA5 regions that are highly conserved throughout evolution (Figure 1). A total of 15 independent variants were identified by WES. Individual 13 is homozygous for the c.989_991del (p.Thr330del) in-frame deletion variant, which is a deletion of the highly evolutionarily conserved threonine 330 and was previously reported by Xu and colleagues[3] as a de novo pathogenic variant in a schizophrenia child-parent trio. Notably, there is no known family history of mental illness in the parents of our individual, suggesting that this variant alone might not be the cause of the schizophrenia in the subject reported by Xu et al.[3] Nine of the variants are nonsynonymous missense substitutions and occur in highly conserved regions of SPATA5; two occur in AAA domains, and three occur in the CDC48 N-terminal domain, an evolutionarily conserved substrate recognition domain that binds to polypeptides, prevents protein aggregation, and is involved in protein folding. The recurrent p.Arg186* variant in individuals 4 and 5 is part of a common haplotype, and the arginine 186 residue is located within a putative ubiquitylation site in SPATA5. The two frameshift variants affecting the AAA domains—p.Arg186* and splice-site variant c.1714+1G>A—are predicted to disrupt or cause loss of protein function through either nonsense-mediated mRNA decay or protein truncation.

SPATA5 is located in chromosomal region 4q28.1 and encodes a member of the AAA protein family. AAA family members are defined by a highly conserved ATPase domain, which is involved in a variety of cellular processes, including protein unfolding and degradation, microtubule motor movement, DNA replication, and membrane fusion. Pathogenic variants in AAA proteins lead to various disorders, including hereditary spastic paraplegia (MIM: 607259), Zellweger syndrome (MIM: 214100), early-onset torsion dystonia (MIM: 605204), and Paget disease with frontotemporal dementia (MIM: 601023). Hereditary spastic paraplegia results from auto-somal-dominant gene-disrupting mutations affecting the AAA domain of spastin, a microtubule regulator, or from a variety of autosomal-recessive mutations, including frameshift insertion-deletions, splice-site mutations, missense mutations, and nonsense mutations in the para-plegin gene, which encodes a mitochondrial protease. Zell-weger syndrome is caused by mutations in genes encoding peroxisomal matrix proteins. The most common sequence change is p.Gly843Asp (c.2528G>A) in PEX1, which is responsible for over a third of cases. Early-onset torsion dystonia is the result of a single amino acid deletion in torsinA, an endoplasmic reticulum lumen protein. Paget disease with frontotemporal dementia results from missense variants in p97, an abundant AAA protein involved in cellular activities such as ER membrane protein degradation and ubiquitin homeostasis.[14,15]

SPATA5 is an 892-amino-acid protein first identified in mouse testes as a spermatogenesis associated factor (SPAF) that might be involved in regulating the structural integrity of mitochondria during spermatogenesis.[16] SPATA5 consists of a putative mitochondrial targeting sequence and two AAA domains and is expressed ubiquitously, including in the testes, spleen, skin, intestines, and brain. Paraplegin, an AAA protein similar to SPATA5, is an ATP-dependent component of a mitochondrial protease complex and is altered in individuals with complex hereditary spastic paraplegia.[17] Paraplegin is required for ribosome assembly and translation in mitochondria. Loss-of-function autosomal-recessive pathogenic variants in paraplegin result in a complex I deficiency and increased sensitivity to oxidative stress.[18,19] Another AAA family member, Lon, is a proteolytic ATPase that influences mitochondrial and respiratory function. Homozygous and compound-heterozygous mutations in LONP1 cause cerebral, ocular, dental, auricular, skeletal (CODAS) syndrome, characterized by developmental delay, hearing loss, skeletal defects, and craniofacial anomalies.[20] Although the specific function of SPATA5 is unknown, one possible role for SPATA5 is in mitochondrial integrity and function and would explain the predominant neurological

Figure 1. Variants in SPATA5

(A) Diagram of SPATA5 with variants identified in green. Missense and in-frame deletions are shown below, and gene-disrupting variants are shown above.

(B) Sequence alignment of the CDC48 N-terminal domain (turquoise), AAA domains (yellow), and Walker A, Walker B, and second region of homology (SRH) motifs (blue text, underlined). A putative mitochondria-targeting sequence is highlighted in green, and potential ubiquitination sites[11–13] are in gray. Residues altered in (A) are shown in bold red text. Species abbreviations are as follows: chimpanzee (Pantr, *Pan troglodytes*), fruit fly (Drome, *Drosophila melanogaster*), nematode (Cael, *C. elegans*), and budding yeast (Yeast, *S. cerevisiae*).

phenotype. It has been suggested that SPATA5 is involved in the morphological transformation of mitochondria from an "orthodox" to a "condensed" form, which occurs during differentiation in spermatogenesis and might be a mechanism to compensate for the thermodynamically unfavorable conditions and decreased oxygen supply due to the blood-testis barrier for differentiating cells in the adluminal compartment. Mitochondrial morphogenesis plays an important role in synaptic development and plasticity, and disruptions in this process are associated with neurodegenerative disorders.[21,22] The abnormally shaped mitochondria in individuals 3 and 14 might be due to defects in SPATA5 function.

Functional assays in yeast have shown that the yeast homolog Afg2 (ATPase family gene) is essential for the release and recycling of nucleolar shuttling factors from pre-60S ribosomal particles.[23,24] AAA proteins act as chaperones that bind and change the conformation of substrates during their ATPase cycle. Upon binding ATP and hydrolysis, the force generated by an AAA protein is propagated to its bound substrates and thus allows the ATP-dependent structural or conformational change of the substrate, resulting in translocation or remodeling and unfolding or disassembly of protein complexes.[15] Heallen and colleagues[25] showed that the C. elegans gene cdc-48.3 is closely related to yeast AFG2 and mammalian SPATA5 and regulates the stability, activity, and localization of aurora B kinase AIR-2 during embryonic development. Aurora B kinase is a highly conserved member of the aurora kinase family of serine threonine kinases and is a key regulator of mitosis. The authors reported that depletion of CDC-48.3 leads to mitotic delays and spindle defects and revealed through site-directed mutagenesis studies that negative regulation of AIR-2 activity occurs by binding of the CDC-48.3 N terminus to AIR-2 and is also dependent on the ATPase activity of CDC-48.3. Proteins involved in the proper alignment of the mitotic spindle are important for maintaining symmetric and asymmetric cell divisions and for controlling cell proliferation. Spindle orientation defects have been associated with neurological and brain diseases, including lissencephaly and primary microcephaly,[26] and therefore could also account for the congenital microcephaly observed in individuals with SPATA5 mutations.

SPATA5 is developmentally expressed throughout the brain, including in the cerebral cortex and hippocampus,[27,28] and might play a critical role in neuronal development and growth. Disrupted mitochondrial morphogenesis during development might lead to neurological disorders, including cognitive impairment, behavioral deficits, and motor sensory dysfunction, as a result of defects in specific neural circuitry. Functional studies of SPATA5 are necessary for determining its role in various cellular processes, especially in the brain, and further investigation of individuals with SPATA5 mutations is essential for elucidating the correlation between genotype and phenotype.

Accession Numbers

Supplemental Data

Supplemental Data include two figures and two tables and can be found with this article online at http://dx.doi.org/10.1016/j.ajhg.2015.07.014.

Acknowledgments

Web Resources

The URLs for data presented herein are as follows:

1000 Genomes, http://www.1000genomes.org/
dbSNP, http://www.ncbi.nlm.nih.gov/SNP/
ExAC Browser, http://exac.broadinstitute.org
NHLBI Exome Sequencing Project (ESP) Exome Variant Server, http://evs.gs.washington.edu/EVS/
GeneMatcher, https://www.genematcher.org
OMIM, http://www.omim.org/

References

1. Yang, Y., Muzny, D.M., Xia, F., Niu, Z., Person, R., Ding, Y., Ward, P., Braxton, A., Wang, M., Buhay, C., et al. (2014). Molecular findings among patients referred for clinical whole-exome sequencing. JAMA 312, 1870–1879.

2. Gilissen, C., Hehir-Kwa, J.Y., Thung, D.T., van de Vorst, M., van Bon, B.W., Willemsen, M.H., Kwint, M., Janssen, I.M., Hoischen, A., Schenck, A., et al. (2014). Genome sequencing identifies major causes of severe intellectual disability. Nature 511, 344–347.

3. Xu, B., Roos, J.L., Dexheimer, P., Boone, B., Plummer, B., Levy, S., Gogos, J.A., and Karayiorgou, M. (2011). Exome sequencing supports a de novo mutational paradigm for schizophrenia. Nat. Genet. 43, 864–868.

4. Allen, A.S., Berkovic, S.F., Cossette, P., Delanty, N., Dlugos, D., Eichler, E.E., Epstein, M.P., Glauser, T., Goldstein, D.B., Han, Y., et al.; Epi4K Consortium; Epilepsy Phenome/Genome Project (2013). De novo mutations in epileptic encephalopathies. Nature 501, 217–221.

5. Yang, Y., Muzny, D.M., Reid, J.G., Bainbridge, M.N., Willis, A., Ward, P.A., Braxton, A., Beuten, J., Xia, F., Niu, Z., et al. (2013). Clinical whole-exome sequencing for the diagnosis of mendelian disorders. N. Engl. J. Med. *369*, 1502–1511.

6. Sobreira, N., Schiettecatte, F., Boehm, C., Valle, D., and Hamosh, A. (2015). New tools for Mendelian disease gene identification: PhenoDB variant analysis module; and GeneMatcher, a web-based tool for linking investigators with an interest in the same gene. Hum. Mutat. *36*, 425–431.

7. Li, H., and Durbin, R. (2009). Fast and accurate short read alignment with Burrows-Wheeler transform. Bioinformatics *25*, 1754–1760.

8. Li, H. (2012). Exploring single-sample SNP and INDEL calling with whole-genome de novo assembly. Bioinformatics *28*, 1838–1844.

9. DePristo, M.A., Banks, E., Poplin, R., Garimella, K.V., Maguire, J.R., Hartl, C., Philippakis, A.A., del Angel, G., Rivas, M.A., Hanna, M., et al. (2011). A framework for variation discovery and genotyping using next-generation DNA sequencing data. Nat. Genet. *43*, 491–498.

10. Li, H., Handsaker, B., Wysoker, A., Fennell, T., Ruan, J., Homer, N., Marth, G., Abecasis, G., and Durbin, R.; 1000 Genome Project Data Processing Subgroup (2009). The Sequence Alignment/Map format and SAMtools. Bioinformatics *25*, 2078–2079.

11. Ren, R.J., Dammer, E.B., Wang, G., Seyfried, N.T., and Levey, A.I. (2014). Proteomics of protein post-translational modifications implicated in neurodegeneration. Transl. Neurodegener. *3*, 23.

12. Stes, E., Laga, M., Walton, A., Samyn, N., Timmerman, E., De Smet, I., Goormachtig, S., and Gevaert, K. (2014). A COFRADIC protocol to study protein ubiquitination. J. Proteome Res. *13*, 3107–3113.

13. Wagner, S.A., Beli, P., Weinert, B.T., Nielsen, M.L., Cox, J., Mann, M., and Choudhary, C. (2011). A proteome-wide, quantitative survey of in vivo ubiquitylation sites reveals widespread regulatory roles. Mol. Cell. Proteomics *10*, M111.013284.

14. Hanson, P.I., and Whiteheart, S.W. (2005). AAA+ proteins: have engine, will work. Nat. Rev. Mol. Cell Biol. *6*, 519–529.

15. Sauer, R.T., and Baker, T.A. (2011). AAA+ proteases: ATP-fueled machines of protein destruction. Annu. Rev. Biochem. *80*, 587–612.

16. Liu, Y., Black, J., Kisiel, N., and Kulesz-Martin, M.F. (2000). SPAF, a new AAA-protein specific to early spermatogenesis and malignant conversion. Oncogene *19*, 1579–1588.

17. van Gassen, K.L., van der Heijden, C.D., de Bot, S.T., den Dunnen, W.F., van den Berg, L.H., Verschuuren-Bemelmans, C.C., Kremer, H.P., Veldink, J.H., Kamsteeg, E.J., Scheffer, H., and van de Warrenburg, B.P. (2012). Genotype-phenotype correlations in spastic paraplegia type 7: a study in a large Dutch cohort. Brain *135*, 2994–3004.

18. Casari, G., De Fusco, M., Ciarmatori, S., Zeviani, M., Mora, M., Fernandez, P., De Michele, G., Filla, A., Cocozza, S., Marconi, R., et al. (1998). Spastic paraplegia and OXPHOS impairment caused by mutations in paraplegin, a nuclear-encoded mitochondrial metalloprotease. Cell *93*, 973–983.

19. Elleuch, N., Depienne, C., Benomar, A., Hernandez, A.M., Ferrer, X., Fontaine, B., Grid, D., Tallaksen, C.M., Zemmouri, R., Stevanin, G., et al. (2006). Mutation analysis of the paraplegin gene (SPG7) in patients with hereditary spastic paraplegia. Neurology *66*, 654–659.

20. Strauss, K.A., Jinks, R.N., Puffenberger, E.G., Venkatesh, S., Singh, K., Cheng, I., Mikita, N., Thilagavathi, J., Lee, J., Sarafianos, S., et al. (2015). CODAS syndrome is associated with mutations of LONP1, encoding mitochondrial AAA+ Lon protease. Am. J. Hum. Genet. *96*, 121–135.

21. Mattson, M.P., Gleichmann, M., and Cheng, A. (2008). Mitochondria in neuroplasticity and neurological disorders. Neuron *60*, 748–766.

22. Völgyi, K., Gulyássy, P., Háden, K., Kis, V., Badics, K., Kékesi, K.A., Simor, A., Györffy, B., Tóth, E.A., Lubec, G., et al. (2015). Synaptic mitochondria: a brain mitochondria cluster with a specific proteome. J. Proteomics *120*, 142–157.

23. Pertschy, B., Saveanu, C., Zisser, G., Lebreton, A., Tengg, M., Jacquier, A., Liebminger, E., Nobis, B., Kappel, L., van der Klei, I., et al. (2007). Cytoplasmic recycling of 60S preribosomal factors depends on the AAA protein Drg1. Mol. Cell. Biol. *27*, 6581–6592.

24. Loibl, M., Klein, I., Prattes, M., Schmidt, C., Kappel, L., Zisser, G., Gungl, A., Krieger, E., Pertschy, B., and Bergler, H. (2014). The drug diazaborine blocks ribosome biogenesis by inhibiting the AAA-ATPase Drg1. J. Biol. Chem. *289*, 3913–3922.

25. Heallen, T.R., Adams, H.P., Furuta, T., Verbrugghe, K.J., and Schumacher, J.M. (2008). An Afg2/Spaf-related Cdc48-like AAA ATPase regulates the stability and activity of the C. elegans Aurora B kinase AIR-2. Dev. Cell *15*, 603–616.

26. Noatynska, A., Gotta, M., and Meraldi, P. (2012). Mitotic spindle (DIS)orientation and DISease: cause or consequence? J. Cell Biol. *199*, 1025–1035.

27. Miller, J.A., Ding, S.L., Sunkin, S.M., Smith, K.A., Ng, L., Szafer, A., Ebbert, A., Riley, Z.L., Royall, J.J., Aiona, K., et al. (2014). Transcriptional landscape of the prenatal human brain. Nature *508*, 199–206.

28. Hawrylycz, M.J., Lein, E.S., Guillozet-Bongaarts, A.L., Shen, E.H., Ng, L., Miller, J.A., van de Lagemaat, L.N., Smith, K.A., Ebbert, A., Riley, Z.L., et al. (2012). An anatomically comprehensive atlas of the adult human brain transcriptome. Nature *489*, 391–399.